Supporting Information

Article title: **Mp*TCP1* controls cell proliferation and redox processes in *Marchantia polymorpha***

Authors: Andrea Busch, Marek Deckena, Marilia Almeida-Trapp, Sarah Kopischke, Cilian Kock, Esther Schüssler, Miltos Tsiantis, Axel Mithöfer, Sabine Zachgo

Fig. S1 Genome-editing of the Mp*TCP1* locus to generate Mp*TCP1* knockout mutants in *Marchantia polymorpha*.

Fig. S2 UV chromatogram and MS analyses for riccionidin detection in Marchantia.

Fig. S3 SDS gel and Western blot.

Fig. S4 Gametangiophore phenotypes of male and female *Marchantia polymorpha* Mp*tcp1*^{ge} lines.

Fig. S5 Comparison of Mp*TCP1* expression in vegetative and sexual Marchantia tissues.

Fig. S6 Effect of 3-AT on gemmae growth.

Fig. S7 Loss of Mp*TCP1* function does not result in pigment synthesis and H_2O_2 accumulation in Mp*tcp1*^{ge} archegoniophores.

Table S1 List of all primer sequences used in the study.

Table S2 Quantification of reduced thallus growth observed in Mp*tcp1*^{ge} lines.

Table S3 List of accession numbers from gene groups involved in ROS metabolism or pigment synthesis from all differentially expressed genes responding to loss of Mp*TCP1* function.

Table S4 Quantification of reduced thallus growth of Marchantia wild-type gemmae grown on 3-AT.

Table S5 Metabolome analysis of Mp*tcp1*^{ge} lines.

Methods S1 Additional methodological details are given for data presented in Figs S1 – S7.

Fig. S1 Genome-editing of the Mp*TCP1* locus to generate Mp*TCP1* knockout mutants in *Marchantia polymorpha*. (a) Schematic representation of the Mp*TCP1* locus (Mapoly0068s0102) obtained from *M. polymorpha* ssp. *ruderalis*, ecotype BoGa, depicts the 1,608 nt long coding sequence (CDS, black), including the TCP domain (blue), the 1,560 nt long 5' UTR (untranslated region) and the 1,639 nt long 3' UTR (both in green). UTRs were determined according to RNA-Seq read alignments from wild-type thallus samples. Red lines indicate the two gRNA binding sites used for knockout mutant generation by a double CRISPR/Cas9 approach. The target site for the TALEN approach is marked by a red triangle. Respective nucleotide positions are indicated. The triplet encoding the conserved cysteine at amino acid position 131 (Cys131) is indicated with a black line. (b) Alignment of the wild-type Mp*TCP1* locus and five analyzed Mp*tcp1*^{ge} lines obtained via the CRISPR/Cas9 approach. The number of deleted nucleotides is given for each line. Sequences of gRNAs are shown in red and nt positions corresponding to the representation in (a) are indicated. Triangles mark additional nucleotide insertions: *GGTGTGTATCCATCCAGTGTTTCATTGCAC; **CAATATCACATTAACAATCA-TAATATCCAC. For four lines (Mp*tcp1-1/3/4/5*^{ge}), the complete CDS was removed. Mp*tcp1-2*^{ge} still comprises 342 nt from the 5' CDS including the first 10 nt from the TCP domain before the deletion occurred (blue). (c) Alignment of TCP domain sequences from five knockout lines generated with the TALEN technique. The position and length of deletions/insertions in the TCP domain that lead to a frame shift in the Mp*TCP1* open reading frame generating premature stop-codons causing truncated proteins are indicated. Binding sites of the effector proteins are underlined. (d) Determination of surface areas of six wild-type (WT) and the five TALEN Mp*tcp1*^{ge} lines measured 12 days after germination (DAG). Error bars display ± SD and average values for each line derive from analysis of at least 8 plants. Scale bar: 5 mm. (e) Thallus of 22 DAG wild-type, Mp*tcp1-1*^{ge} and a Mp*tcp1-1*^{ge} plant that carries the Mp*EF1a*:Mp*TCP1* construct. Thallus growth in Mp*tcp1-1*^{ge} is greatly reduced compared to wild-type (see Fig. 1) and the growth deficiency can be rescued upon transformation of Mp*tcp1-1*^{ge} with the pMp*EF1a*:Mp*TCP1* construct. Scale bar: 5 mm.

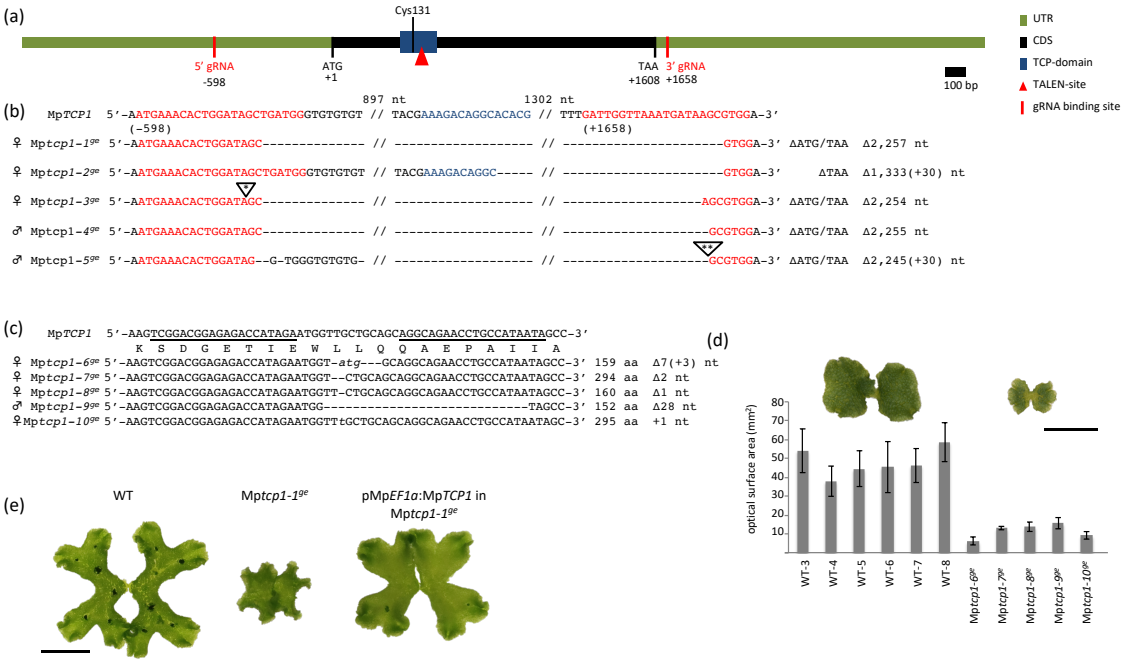
(a)
Cys131
5′ gRNA
-598
ATG
+1
TAA
+1608
3′ gRNA
+1658
100 bp
UTR
CDS
TCP-domain
TALEN-site
gRNA binding site
(b)
MpTCP1 5′-AATGAAACACTGGATAGCTGATGGGTGTGTGT // TACGAAAGACAGGCACACG // TTTGATTGGTTAAATGATAAGCGTGGA-3′
(−598)
897 nt
1302 nt
(+1658)
♀ Mptcp1-1ge 5′-AATGAAACACTGGATAGC---------- // ---------- // ----------GTGGA-3′ ΔATG/TAA Δ2,257 nt
♀ Mptcp1-2ge 5′-AATGAAACACTGGATAGCTGATGGGTGTGTGT // TACGAAAGACAGGC----- // ----------GTGGA-3′ ΔTAA Δ1,333(+30) nt
♀ Mptcp1-3ge 5′-AATGAAACACTGGATAGC---------- // ---------- // ----------AGCGTGGA-3′ ΔATG/TAA Δ2,254 nt
♂ Mptcp1-4ge 5′-AATGAAACACTGGATAGC---------- // ---------- // ----------GCGTGGA-3′ ΔATG/TAA Δ2,255 nt
♂ Mptcp1-5ge 5′-AATGAAACACTGGATAG--G-TGGGTGTGTG- // ---------- // ----------GCGTGGA-3′ ΔATG/TAA Δ2,245(+30) nt
(c)
MpTCP1 5′-AAGTCGGACGGAGAGACCATAGAATGGTTGCTGCAGCAGGCAGAACCTGCCATAATAGCC-3′
K S D G E T I E W L L Q Q A E P A I I A
♀ Mptcp1-6ge 5′-AAGTCGGACGGAGAGACCATAGAATGGT-atg---GCAGGCAGAACCTGCCATAATAGCC-3′ 159 aa Δ7(+3) nt
♀ Mptcp1-7ge 5′-AAGTCGGACGGAGAGACCATAGAATGGT--CTGCAGCAGGCAGAACCTGCCATAATAGCC-3′ 294 aa Δ2 nt
♀ Mptcp1-8ge 5′-AAGTCGGACGGAGAGACCATAGAATGGTT-CTGCAGCAGGCAGAACCTGCCATAATAGCC-3′ 160 aa Δ1 nt
♂ Mptcp1-9ge 5′-AAGTCGGACGGAGAGACCATAGAATGG----------TAGCC-3′ 152 aa Δ28 nt
♀ Mptcp1-10ge 5′-AAGTCGGACGGAGAGACCATAGAATGGTTtGCTGCAGCAGGCAGAACCTGCCATAATAGC-3′ 295 aa +1 nt
(d)
optical surface area (mm²)
80
70
60
50
40
30
20
10
WT-3
WT-4
WT-5
WT-6
WT-7
WT-8
Mptcp1-6ge
Mptcp1-7ge
Mptcp1-8ge
Mptcp1-9ge
Mptcp1-10ge
(e)
WT
Mptcp1-1ge
pMpEF1α:MpTCP1 in Mptcp1-1ge

Fig. S2 UV chromatogram and MS analyses for riccionidin detection in Marchantia. (a-c) HPLC-DAD-HRMS analysis was conducted with stressed wild-type (WT) plants, shown to accumulate visual amounts of the red pigment riccionidin when grown on minimal nutrient medium (Albert *et al.*, 2018). Samples were extracted using MeOH : H_2O : HCl (1 : 1 : 0.02). (a) The UV chromatogram at 480 nm, the absorption wavelength of riccionidin, shows an intense band at 5.7 min in the extracts from stressed wild-type plants. (b) The UV spectrum (upper panel) reveals major absorbance at 284 and at 492 nm and the MS spectrum (lower panel) determines a *m/z* of 285.0394 associated to this peak (see (a)), indicating that it is related to riccionidin (Kunz *et al.*, 1994; Albert *et al.*, 2018) and that the applied method is suitable for detection of riccionidin. (c) A selected ion chromatogram of *m/z* 285.0394 detects one peak related to riccionidin at 5.7 min in extracts from stressed wild-type plants. (d) Whereas red pigments are visible in extracts from stressed wild-type plants, the extract from Mp*tcp1*^{ge} plants remains light green. (e) UV chromatogram at 480 nm and (f) selected ion chromatogram of *m/z* 285.0394 of wild-type and Mp*tcp1*^{ge} plants. Differently from the analysis of stressed wild-type plants (see (a)), no peak could be detected at 5.7 min in the UV chromatogram of extracts from non-stressed wild-type and Mp*tcp1*^{ge} plants. Only the more sensitive selected ion chromatogram (f) detects a peak for riccionidin at 5.7 min in extracts from Mp*tcp1*^{ge} and wild-type plants. (g) Relative quantification of riccionidin in wild-type and Mp*tcp1*^{ge} plants based on the more sensitive selected ion chromatogram (see (f)) shows a 15.6-fold increase of riccionidin content in Mp*tcp1*^{ge} compared to wild-type plants (see also Table S5), implying that Mp*TCP1* represses riccionidin formation in wild-type plants. Error bars display standard deviations and p-value was determined by Student's t-test (* $P < 0.05$).

To conclude, despite a 15.6-fold riccionidin increase in Mp*tcp1*^{ge} plants compared to non-stressed wild-type plants, this pigment is likely not present in Mp*tcp1*^{ge} plants in sufficiently high amounts to contribute to the observed red pigmentation for the following reasons: With the riccionidin-extraction method, no visible pigment could be extracted from Mp*tcp1*^{ge} plants, only from stressed wild-type plants. Moreover, we could not detect a riccionidin specific peak in the UV chromatogram made from Mp*tcp1*^{ge} plants (see (e)). Finally, although the more sensitive selected ion chromatogram could detect riccionidin in Mp*tcp1*^{ge} plants, riccionidin amounts are 34-fold lower in Mp*tcp1*^{ge} plants compared to

extracts from stressed wild-type plants (compare (c) and (f)), where pigment was visible in extracts. Thus, riccionidin likely does not significantly contribute to the red pigmentation observed in Mp*tcp1*^{ge} plants. Int.: Intensity; mAU: milli absorbance units; *m/z*: mass divided by charge number of ions; λ: wavelength.

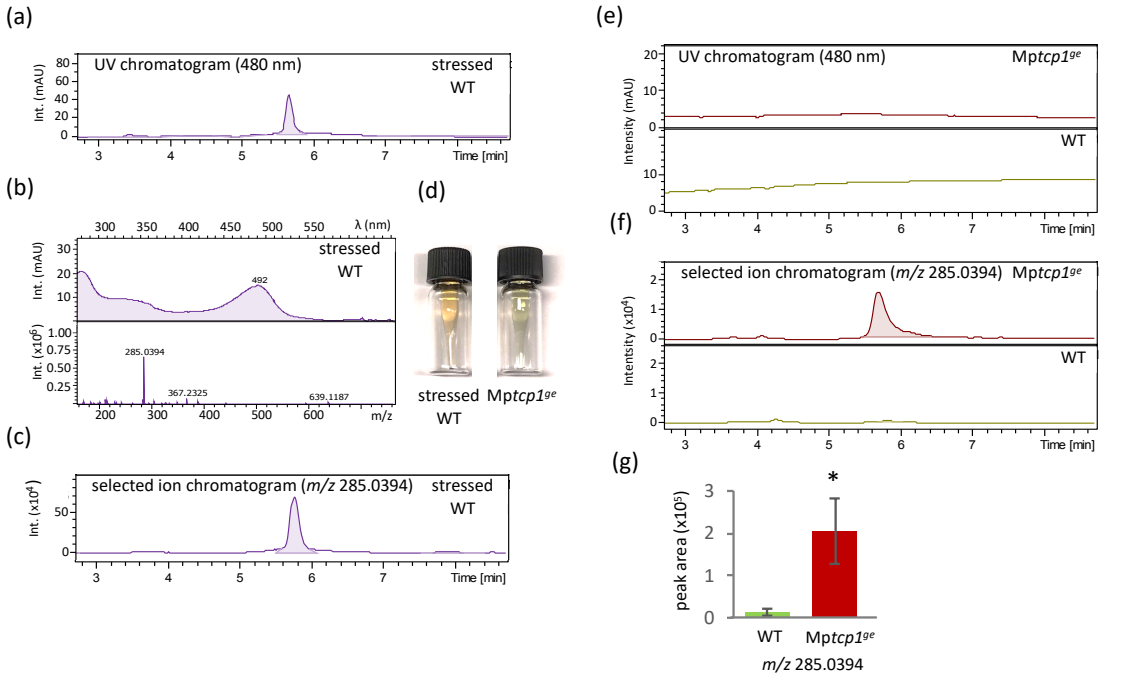

Fig. S3 SDS gel and Western blot. (a) SDS gel and (b) Western blot analysis of recombinant MBP (maltose binding protein)-MpTCP1 (lane 1), MBP-MpTCP1C131S (lane 2) proteins and MBP alone (lane 3), the latter was used as a control in EMSA analysis. Red arrows indicate MpTCP1 and MpTCP1C131S protein bands with a size of 102 kDa. Arrowheads indicate MBP protein with a size of 43 kDa. The band below MBP (asterisk) is likely a degraded form of MBP. Prestained protein ladder is shown on the left.

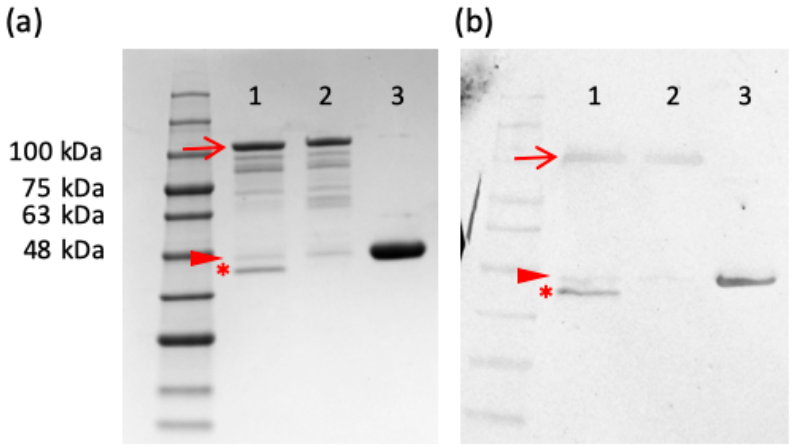

Fig. S4 Gametangiophore phenotypes of male and female *Marchantia polymorpha* Mp*tcp1*^{ge} lines. (a) Archegoniophores of wild-type (WT) and Mp*tcp1-3*^{ge} plants. The stalks of Mp*tcp1*^{ge} archegoniophores are shorter and rays are irregularly sized and shaped compared to wild-type plants. The inset magnifies a Mp*tcp1-3*^{ge} archegoniophore revealing additional archegoniophore tissue formation protruding between the rays (arrow). (b) Antheridiophores of wild-type and Mp*tcp1-4*^{ge} plants, with magnification of Mp*tcp1-4*^{ge} in inset. Antheridiophores reveal abnormalities similar to mutant archegoniophores, with the development of shorter stalks and the occasional outgrowth of lobes, forming protrusions that are indicated by arrowheads in (e). Overall, capitula are smaller compared to wild-type plants. Images (a,b) show side (upper row) and top views (lower row). (c) Side view of three archegoniophores from CRISPR/Cas9 and (d) from TALEN generated Mp*tcp1*^{ge} knockout (KO) lines. Antheridiophores of CRISPR/Cas9 generated male Mp*tcp1-5*^{ge} line (e) and the TALEN generated line Mp*tcp1-9*^{ge} (f). (e,f). Left: side view, right: top view. Scale bars: 2 mm.

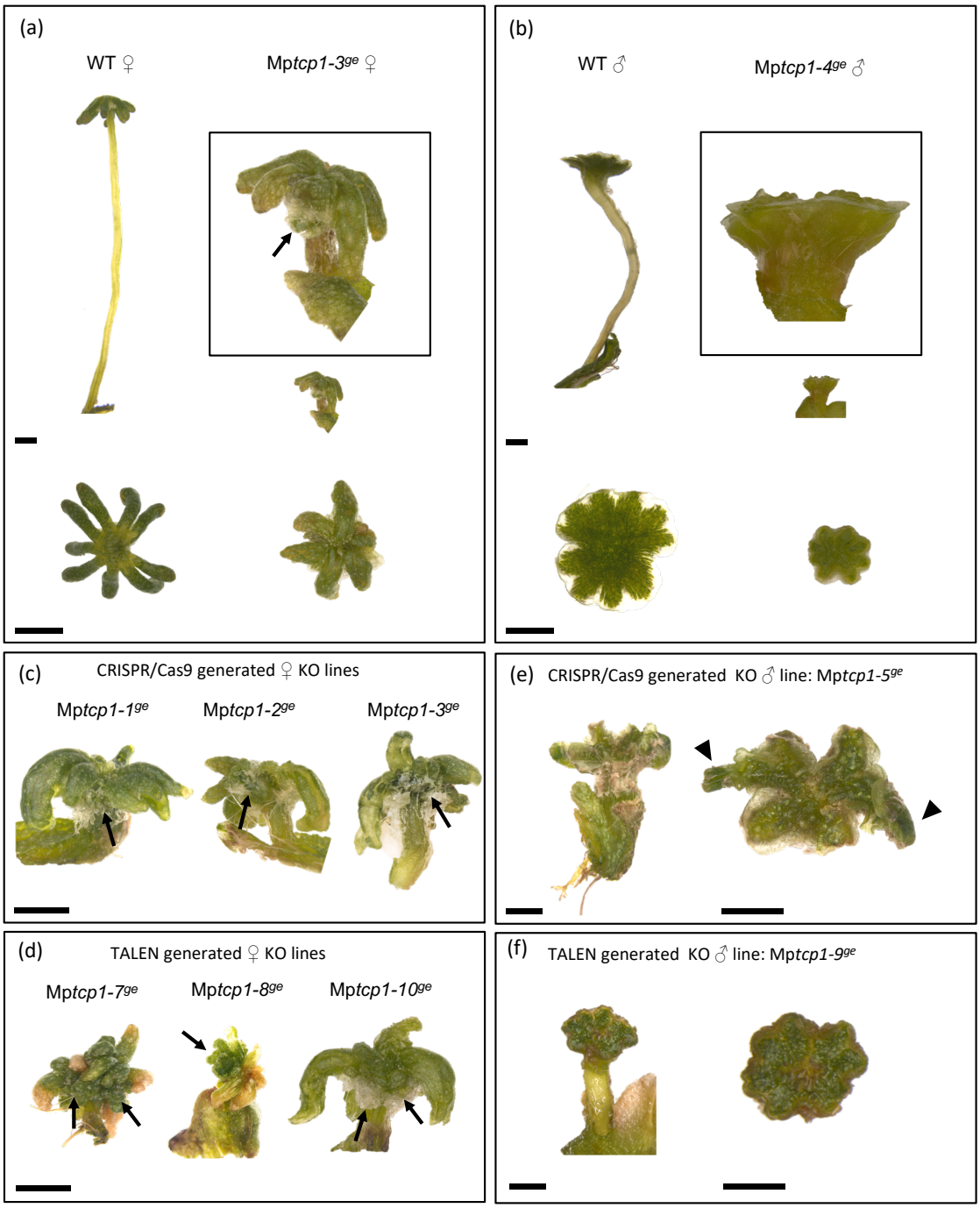
(a)
WT ♀
Mp*tcp1-3*^{ge} ♀
(b)
WT ♂
Mp*tcp1-4*^{ge} ♂
(c)
CRISPR/Cas9 generated ♀ KO lines
Mp*tcp1-1*^{ge}
Mp*tcp1-2*^{ge}
Mp*tcp1-3*^{ge}
(e)
CRISPR/Cas9 generated KO ♂ line: Mp*tcp1-5*^{ge}
(d)
TALEN generated ♀ KO lines
Mp*tcp1-7*^{ge}
Mp*tcp1-8*^{ge}
Mp*tcp1-10*^{ge}
(f)
TALEN generated KO ♂ line: Mp*tcp1-9*^{ge}

Fig. S5 Comparison of Mp*TCP1* expression in vegetative and sexual Marchantia tissues. (a) Semi-quantitative RT-PCR analysis in different tissues of *M. polymorpha* ssp. *ruderalis*, ecotype BoGa. For quantification of Mp*TCP1* transcript abundance, expression in each sample was normalized against that of Mp*EF1α* (Mapoly0024s0116). Error bars display ± SD, average values are based on two technical replicates. Me, meristematic region; th, thallus; gc, gemma cup; Ag, archegoniophore; At, antheridiophore; S1, young gametangiophore; S2, medium stage gametangiophore; S3, mature gametangiophore; Sp, sporeling. (b) Relative expression data of Mp*TCP1* (Mapoly0068s0102, ver. 3.1) from the marchantia.info web site. Expression was deduced from FPKM values from RNA-Seq experiments (Bowman *et al.*, 2017), conducted with male and female Marchantia TAK1 ecotype (HATP: TAK1 thalli, cut 0 hrs, SRR896229; HATS: antheridiophores, SRR896230; HAUC: sporophytes, SRR896223; HATG: archegoniophores, SRR896225).

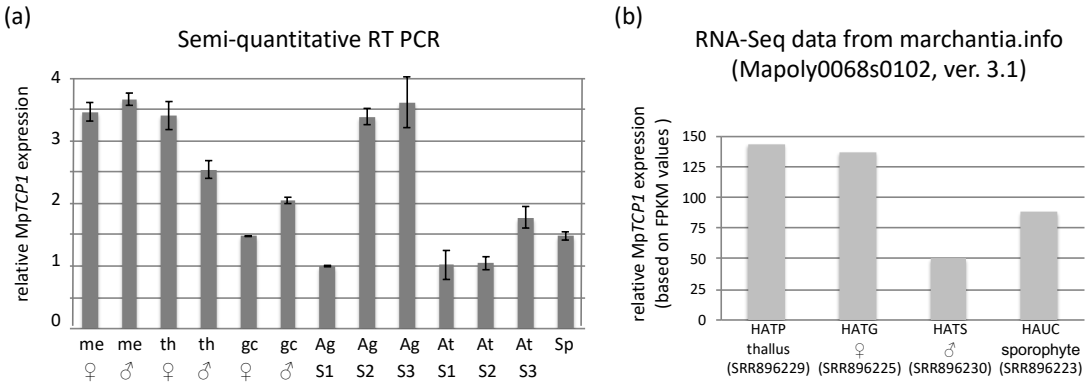

Fig. S6 Effect of 3-AT on gemmae growth. Marchantia gemmae were cultivate on normal medium and medium supplemented with 25 µM, 50 µM, 100 µM, 200 µM or 400 µM 3-AT (3-amino-1,2,4-triazole) for 9 DAG (days after germination). A clearly discernible growth effect was first observed for 100 µM 3-AT treatment and therefore this concentration was used for further experiments. (a) Determination of H_2O_2 from extracts of gemmae 9 DAG grown on medium supplemented with 100 µM 3-AT and on normal (mock) medium revealed a 1.9-fold H_2O_2 increase in 3-AT-treated gemmae. Average values are derived from 5 wild-type lines for each condition, measurements were repeated three times. (b) The surface area of complete gemmae from wild-type lines grown on 3-AT medium and on mock medium was determined at 3, 7, 12 and 17 DAG causing a 1.7 to 2.3-fold growth retardation compared to gemmae of the same age grown on mock medium (see Table S4). Average values are derived from 8 lines with at least 54 gemmae for each condition. All error bars display ± SD and p-values were determined by Student's t-test (*** $P < 0.001$, * $P < 0.05$, ns: not significant).

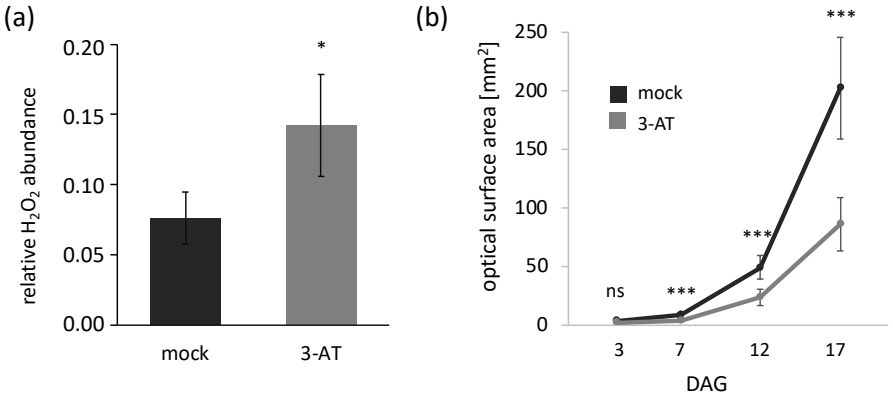

Fig. S7 Loss of Mp*TCP1* function does not result in pigment synthesis and H_2O_2 accumulation in Mp*tcp1*^{ge} archegoniophores. (a) Determination of H_2O_2 in extracts from Marchantia wild-type (WT) and Mp*tcp1*^{ge} archegoniophores using potassium iodide staining. Average values are derived from three independent wild-type and Mp*tcp1*^{ge} line measurements. Error bars display ± SD and p-values, determined by Student's t-test, did not indicate significant differences (ns). (b) Both, wild-type and Mp*tcp1-1*^{ge} archegoniophores do not reveal pigmentation after clearance with methanol. Scale bar: 2 mm. (c) Differentially expressed gene (DEG) groups with a putative function in ROS metabolism or pigment synthesis obtained from comparisons of Mp*tcp1*^{ge} vs wild-type thalli and archegoniophores transcriptomes (fold change (FC) ≥ 2; adjusted p-value < 0.0001). Putative gene functions are based on Marchantia functional gene annotations, downloaded from marchantia.info and/or sequence comparison with *Arabidopsis thaliana* using BLAST2.2.8 provided by TAIR (www.arabidopsis.org/index.jsp). A list with all accessions from the gene groups mentioned is given in Table S3a and S3b. C4H: cinnamate 4-hydroxylase; DAHPS: 3-Deoxy-d-arabino-heptulosonate-7-phosphate synthase; DHAR: dehydroascorbate reductase; GSH: glutathione; GSSG: oxidized glutathione disulfide dimer; PPP: phenylpropanoid pathway; PPO: Polyphenol oxidase; PRXIII: class III peroxidase.

(a)

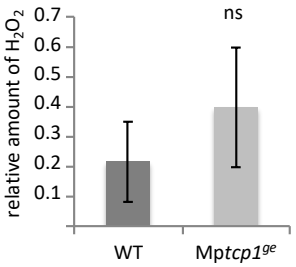

(b)

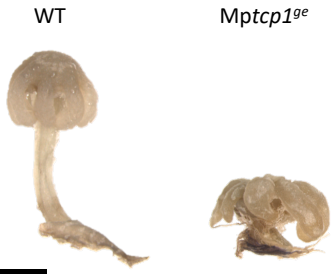

(c)

	Thallus		Archegoniophore		
Annotation	**No. of DEGs**	**FC range (Mp*tcp1*^{ge}/WT)**	**No. of DEGs**	**FC range (Mp*tcp1*^{ge}/WT)**	**Putative metabolic function**
PRXIII	25	2.3 to 20.7	0	-	Apoplastic generation and degradation of H_2O_2 in a substrate-dependent manner
	7	-76.3 to -2.4	5	-2.5 to -6.6	and oxidative coupling of monolignols, precursors in lignan/lignin biosynthesis
Catalase	1	-8.5	0	-	Dismutation of H_2O_2 to H_2O
Copper amine oxidase	1	12.4	0	-	Source of H_2O_2
Polyamine oxidase	2	2.3, 2.5	1	3.2	Source of H_2O_2
Glutathion-*S*-transferase (DHAR class)	2	-5.1, -4.9	0	-	Reduction of dehydroascorbate and concomitant oxidation of GSH to GSSG
Aquaporins	9	2.4 to 20.7	0	-	Transport of H_2O and H_2O_2 across cell membrane into the cytoplasm
Dirigent-like proteins	1	-5.9	3	-2.1 to -4.0	Ensure stereoselectivity of monolignol coupling in lignan/lignin biosynthesis
	8	2.1 to 65.2	0	-	
PPO/tyrosinases	20	3.1 to 334.8	0	-	Synthesis of aminochrome and derivatives by oxidizing the phenolic ring of tyrosine
	0	-	1	-3.4	
Chalcone synthase	1	4.6	0	-	PPP enzyme; synthesis of chalcone, a key step in flavonoid biosynthesis
	0	-	1	-98.4	
C4H	1	3.0	0	-	PPP enzyme; catalysis of the aromatic hydroxylation forming 4-coumarate
DAHPS	1	2.0	0	-	Enzyme of the shikimate pathway, which provides phenylalanine to the PPP

Table S1 List of all primer sequences used in the study.

Sequence 5'-3'	**Use**
gRNA1 and gRNA2 primers for double CRISPR/Cas9	
CTCGATGAAACACTGGATAGCTGA	Forward: *gRNA1* with *Bsa*I site (bold)
AAACTCAGCTATCCAGTGTTTCAT	Reverse: *gRNA1* with *Bsa*I site (bold)
CTCGGATTGGTTAAATGATAAGCG	Forward: *gRNA2* with *Bsa*I site (bold)
AAACCGCTTATCATTTAACCAATC	Reverse: *gRNA2* with *Bsa*I site (bold)
Double CRISPR/Cas9 amplification and sequencing primer	
ATCAGGTCAAGTCTCTGGAAGCGCAAGGAG	Forward: Mp*TCP1* CRISPR/Cas9 verification
GGATCATGATGTTGGTCCGAGATC	Reverse: Mp*TCP1* CRISPR/Cas9 verification
***In situ* hybridization primers**	
ATGTCTGGACGCGGCAA	Forward: Mp*H4*
CTACCCCCCGAACCCG	Reverse: Mp*H4*
ATCAGGTCAAGTCTCTGGAAGCGCAAGGAG	Forward: *MpTCP1*
CGCGTAATACGACTCACTATAGGGTTACTGCGAGCTAGTGGGATC	Reverse: *MpTCP1* with *T7* RNA polymerase promoter sequence (bold)
Mp*TCP1* / Mp*TCP1C131S* amplification and cloning (into pMALc5X) primers for in vitro DNA binding studies	
ACGC**GTCGAC**GGTGTGTGTGCCCCCTTG	Forward: Mp*TCP1* / Mp*TCP1C131S* with *Sal*I (bold)
CCC**AAGCTT**TTACTGCGAGCTAGTG	Reverse: Mp*TCP1* / Mp*TCP1C131S with Hin*dIII (bold)
C131S substitution for pMAL-c5X Mp*TCP1C131S*	
GAGGATTCGAATGCCTGCCTCGTCCGCCGCCCGGATTTTCC	Forward: underlined are the nucleotides encoding for serine
GAGTCAGCTGGAAAATCCGGGCGGCGGACGAGGCAGGCATTC	Reverse: underlined are the nucleotides encoding for serine
DNA binding motifs	
ACTCCATGGTCCCACCCATGGTCCCAC	Forward: site IIb
GTGGGACCATGGGTGGGACCATGGAGT	Reverse: site IIb
ACTCCATGGTCGAACCCATGGTCGAAC	Forward: site IIb mutagenized
GTTCGACCATGGGTTCGACCATGGAGTC	Reverse: site IIb mutagenized
GGTGGGCCCGTAGGTGGGCCCGTA	Forward: site IIa
TACGGGCCCACCTACGGGCCCACC	Reverse: site IIa
GGTGGGCGAGTAGGTGGGCGAGTA	Forward: site IIa mutagenized
TACTCGCCCACCTACTCGCCCACC	Reverse: site IIa mutagenized

Primer sequences used in this study are listed in 5' to 3' orientation together with their designated purpose.

Table S2 Quantification of reduced thallus growth observed in Mp*tcp1*^{ge} lines.

	0 DAG (mm^2)	**1 DAG (mm^2)**	**5 DAG (mm^2)**	**9 DAG (mm^2)**	**12 DAG (mm^2)**
WT	0.38 ± 0.12	0.48 ± 0.14	3.49 ± 1.13	14.14 ± 3.89	43.02 ± 11.44
Mp*tcp1*^{ge}	0.33 ± 0.11	0.36 ± 0.13	1.92 ± 0.47	5.83 ± 1.28	13.02 ± 2.96
Fold change	1.2	1.4	1.8	2.4	3.3

The surface area of Marchantia gemmae from the Mp*tcp1-1/2/3*^{ge} lines and four wild-type (WT) lines was quantified 0, 1, 5, 9 and 12 days after germination (DAG). Average values for each line are based on at least 8 gemmae and standard deviations are given. Fold changes indicate growth reduction observed in Mp*tcp1*^{ge} lines compared to the wild-type.

Table S3 List of accession numbers from gene groups involved in ROS metabolism or pigment synthesis from all differentially expressed genes responding to loss of Mp*TCP1* function.

(a)

ID	Fold change Mp*tcp1*^{ge}/WT	Adjusted p-value	Base mean	Putative gene function
Mapoly0047s0007	2.29	1.27E-06	425.77	Peroxidase
Mapoly0175s0023	2.76	7.36E-08	637.63	Peroxidase
Mapoly0332s0001	3.04	6.19E-07	109.67	Peroxidase
Mapoly0282s0001	3.06	4.60E-06	514.39	Peroxidase
Mapoly0243s0001	3.09	2.63E-06	528.13	Peroxidase
Mapoly0009s0175	3.34	3.95E-20	305.36	Peroxidase
Mapoly0084s0011	3.52	2.32E-08	644.46	Peroxidase
Mapoly0136s0035	3.55	9.90E-13	312.84	Peroxidase
Mapoly0196s0010	3.90	6.32E-12	247.46	Peroxidase
Mapoly0182s0023	4.43	9.78E-08	146.76	Peroxidase
Mapoly0076s0034	7.66	5.20E-26	317.35	Peroxidase
Mapoly0032s0143	15.76	5.86E-10	33.12	Peroxidase
Mapoly0070s0055	2.72	7.13E-06	143.91	Peroxidase
Mapoly0096s0070	2.81	3.59E-12	1689.95	Peroxidase
Mapoly0143s0040	3.00	1.82E-08	274.46	Peroxidase
Mapoly2709s0001	3.16	1.33E-08	238.92	Peroxidase
Mapoly0032s0074	4.33	5.99E-08	134.61	Peroxidase
Mapoly0196s0013	4.48	5.23E-07	125.35	Peroxidase
Mapoly0196s0011	5.33	1.43E-09	96.64	Peroxidase
Mapoly0038s0040	5.68	1.65E-09	596.33	Peroxidase
Mapoly0040s0117	6.70	2.41E-06	67.01	Peroxidase
Mapoly0486s0001	8.89	1.96E-12	111.71	Peroxidase
Mapoly0032s0142	9.10	2.14E-06	83.23	Peroxidase
Mapoly0032s0073	11.19	6.73E-09	61.89	Peroxidase
Mapoly0195s0010	20.68	2.66E-07	19.50	Peroxidase
Mapoly0004s0139	-5.28	2.52E-07	1045.15	Peroxidase
Mapoly0243s0006	-76.26	6.76E-06	13.06	Peroxidase
Mapoly0047s0008	-16.51	3.73E-06	33.98	Peroxidase
Mapoly0064s0029	-6.28	2.16E-21	7547.22	Peroxidase
Mapoly0008s0232	-4.77	1.12E-05	656.73	Peroxidase
Mapoly0002s0115	-3.64	4.55E-05	125.31	Peroxidase
Mapoly0088s0020	-2.40	6.15E-10	299.94	Peroxidase
Mapoly0068s0055	-8.51	1.67E-29	479.02	Catalase

Mapoly0257s0001	12.36	7.93E-05	24.77	Copper Amine Oxidase
Mapoly0001s0321	2.31	7.43E-10	1778.61	Polyamine Oxidases
Mapoly0137s0029	2.49	3.05E-06	241.87	Polyamine Oxidases
Mapoly0085s0095	-5.14	5.17E-08	787.51	GST (DAHR)
Mapoly0019s0024	-4.90	1.37E-22	697.23	GST (DAHR)
Mapoly0002s0018	15.91	4.18E-05	15.60	Aquaporins
Mapoly0001s0424	2.38	1.04E-17	77825.05	Aquaporins
Mapoly0223s0007	3.00	3.86E-15	526.88	Aquaporins
Mapoly0044s0029	5.08	6.06E-13	292.23	Aquaporins
Mapoly0044s0027	20.72	1.94E-06	86.33	Aquaporins
Mapoly0135s0054	2.42	1.45E-07	1045.50	Aquaporins
Mapoly0223s0005	2.78	5.41E-09	171.75	Aquaporins
Mapoly0135s0055	4.36	1.43E-11	832.30	Aquaporins
Mapoly0135s0056	7.20	1.03E-11	113.46	Aquaporins
Mapoly0013s0156	3.54	1.29E-07	115.72	Dirigent-like protein
Mapoly0006s0216	10.56	1.52E-09	582.69	Dirigent-like protein
Mapoly0062s0101	-5.88	2.67E-05	185.45	Dirigent-like protein
Mapoly0009s0115	2.14	1.31E-07	1478.45	Dirigent-like protein
Mapoly0006s0217	3.78	5.26E-06	814.42	Dirigent-like protein
Mapoly0070s0018	4.51	4.54E-05	64.70	Dirigent-like protein
Mapoly0078s0058	4.60	4.13E-08	1102.42	Dirigent-like protein
Mapoly0041s0132	4.80	1.10E-24	897.22	Dirigent-like protein
Mapoly0121s0040	65.22	1.23E-11	221.30	Dirigent-like protein
Mapoly0038s0002	3.08	1.75E-06	123.84	PPO/tyrosinase
Mapoly0071s0078	3.83	5.46E-05	581.07	PPO/tyrosinase
Mapoly0032s0137	4.59	2.06E-07	343.79	PPO/tyrosinase
Mapoly0032s0136	5.64	9.70E-10	428.16	PPO/tyrosinase
Mapoly0038s0112	6.41	1.22E-14	491.43	PPO/tyrosinase
Mapoly0024s0005	10.53	1.11E-10	180.92	PPO/tyrosinase
Mapoly0145s0012	13.88	3.09E-09	41.44	PPO/tyrosinase
Mapoly0134s0001	334.82	4.05E-16	102.07	PPO/tyrosinase
Mapoly3313s0001	3.70	1.13E-11	2083.35	PPO/tyrosinase
Mapoly0654s0001	3.72	5.20E-05	195.80	PPO/tyrosinase
Mapoly0038s0001	4.32	9.45E-07	76.51	PPO/tyrosinase
Mapoly0595s0001	5.01	5.02E-10	319.76	PPO/tyrosinase
Mapoly0084s0022	5.69	8.78E-07	307.30	PPO/tyrosinase
Mapoly0021s0041	13.92	6.84E-15	760.30	PPO/tyrosinase
Mapoly0024s0006	15.57	5.23E-07	27.91	PPO/tyrosinase
Mapoly0145s0009	16.53	6.18E-09	58.90	PPO/tyrosinase
Mapoly0145s0011	62.59	7.68E-15	39.48	PPO/tyrosinase

Mapoly0134s0050	68.60	1.74E-14	126.65	PPO/tyrosinase
Mapoly0266s0004	3.12	2.77E-06	308.97	PPO/tyrosinase
Mapoly0266s0001	3.19	1.44E-07	1183.02	PPO/tyrosinase
Mapoly0072s0061	4.56	2.39E-18	495.59	CHS
Mapoly0081s0009	3.00	3.06E-07	290.39	C4H
Mapoly0008s0188	2.02	2.35E-27	16526.16	DAHPS

(b)

ID	Fold change Mp*tcp1*^{ge}/WT	Adjusted p-value	Base mean	Putative gene function
Mapoly0008s0265	-6.60	1.63E-07	174.29	Peroxidase
Mapoly0088s0020	-5.28	1.49E-33	489.62	Peroxidase
Mapoly0096s0070	-2.54	3.60E-16	1695.28	Peroxidase
Mapoly0067s0039	-6.20	7.06E-06	276.45	Peroxidase
Mapoly0009s0083	-2.58	4.42E-16	1820.36	Peroxidase
Mapoly0099s0017	3.15	1.15E-09	674.17	Polyamine Oxidase
Mapoly0084s0009	-4.04	2.47E-15	992.77	Dirigent-like protein
Mapoly0006s0216	-2.12	3.50E-05	2105.75	Dirigent-like protein
Mapoly0006s0217	-3.43	3.66E-09	983.34	Dirigent-like protein
Mapoly0206s0001	-3.36	7.10E-19	3259.03	PPO/tyrosinase
Mapoly0072s0054	-98.40	4.74E-125	1211.53	CHS

Listed are Marchantia accession numbers from genes that are differentially expressed (a) in the thallus transcriptomes from wild-type (WT) and Mp*tcp1*^{ge} lines and (b) in archegoniophore transcriptomes from wild-type and Mp*tcp1*^{ge} plants. All differentially expressed genes have a fold change ≥ 2 and an adjusted p-value < 0.0001. The putative gene function is based on Marchantia functional gene annotation downloaded from marchantia.info and/or sequence comparison with *Arabidopsis thaliana* using BLAST2.2.8 provided by TAIR (www.arabidopsis.org/index.jsp). C4H: cinnamate 4-hydroxylase; CHS: Chalcone synthase; DAHPS: 3-Deoxy-d-arabino-heptulosonate-7-phosphate synthase; GST: Glutathione-*S*-transferase; PPO: Polyphenol oxidase.

Table S4 Quantification of reduced thallus growth of Marchantia wild-type gemmae grown on 3-AT.

	3 DAG (mm²)	**7 DAG (mm²)**	**12 DAG (mm²)**	**17 DAG (mm²)**
mock	3.50 ± 0.18	8.51 ± 2.12	49.51 ± 10.08	202.30 ± 43.39
3-AT	2.08 ± 0.41	4.42 ± 1.66	23.80 ± 6.97	86.20 ± 22.77
Fold change	1.7	1.9	2.1	2.3

The surface area of gemmae grown on medium supplemented with 100 µM 3-AT (3-amino-1,2,4-triazole) and on mock medium was quantified 3, 7, 12 and 17 days after germination (DAG). Average values derive from 8 lines with at least 54 gemmae for each condition. Standard deviations are given. Fold changes indicate growth reduction observed in 3-AT-treated lines compared to untreated wild-type lines.

Table S5 Metabolome analysis of Mp*tcp1*^{ge} lines.

Compound	Retention time	HRMS	Ionization mode	UV absorption wavelength (intensity)	MS quantification peak area of wild-type (+/- SD)	MS quantification peak area of Mp*tcp1*^{ge} (+/- SD)	MS quantification Fold change
phenylpropanoid	3.4	*m/z* 180.1019	pos	300 (100)	150850 (9229)	546081 (156998)	3.6
aminochrome-derivative 1	6.7	*m/z* 166.0865	pos	300 (100); 484 (35)	273198 (103605)	3008763 (277844)	11.0
aminochrome	11.1	*m/z* 150.0551	pos	302 (100); 420 (38); 484 (38)	268452 (72386)	2393417 (886429)	8.9
aminochrome-derivative 3	13.7	*m/z* 180.0657	pos	290 (100); 484 (58)	793625 (243040)	10473319 (1716439)	13.2
phenylpropanoid	17.7	*m/z* 180.1019	pos	304 (100)	3335 (2140)	1260276 (349423)	377.9
phenylpropanoid	37.8	*m/z* 287.0549	pos	348 (100)	1157760 (346257)	3707202 (796087)	3.2
riccionidin	5.7	*m/z* 285.0394	pos	283(100); 492 (77)	13168 (3369)	204909 (36519)	15.6

Listed are all phenolic compounds that are increased upon loss of Mp*TCP1* function in *Marchantia polymorpha* Mp*tcp1*^{ge} lines with an UV absorption typical for phenylpropanoids. The Mp*tcp1*^{ge} metabolome was analyzed by HPLC-DAD-HRMS, using two different extraction and separation methods for phenylpropanoids/aminochromes and riccionidin (see Material and Methods). Enriched compounds with their respective retention times, molecular ions, ionization mode, spectral characteristics and relative intensities detected by selected ion chromatography based on the given *m/z* values in wild-type and Mp*tcp1*^{ge}, are listed. SD: Standard deviation.

Methods S1 Additional methodological details are given for data presented in Figs S1 – S7.

Complementation of the Mp*tcp1*^{ge} phenotype. For molecular complementation of CRISPR/Cas9-genetrated plants lacking the Mp*TCP1* CDS including adjacent parts of 5' and 3' UTRs, we transformed gemmae of Mp*tcp1-1*^{ge} with a pMp*EF1a*:Mp*TCP1* vector, comprising the complete Mp*TCP1* CDS, including 579 nt of 5' UTR, cloned into pMpGWB403 (Addgene #68668). First, a *Pac*I restriction site was inserted into pMpGWB403, cloning the amplicon generated with forward primer: GGACTAGTCCACAGCATGGCCGTTCATAAGACG and reverse primer: AGAGGAGCTC**TTAATTAA**GCTCGCTCATCGCTCATCCACTCGGTC (*Pac*I site in bold) into pMpGWB403 using *Spe*I and *Sac*I (restriction sites are underlined). Then, the Mp*TCP1* CDS was amplified with forward primer: GGACTAGTATGGGTGTGTGTGCCCCCTTGCCTG (*Spe*I site underlined) and reverse primer: CC**TTAATTAA**TTACTGCGAGCTAGTGGGATCGTCGCC (*Pac*I in bold) and integrated using *Spe*I and *Pac*I. Gemmae transformation was conducted as described by Tsuboyama *et al.* (2018) using *Agrobacterium tumefaciens* strain C58C1.

Extraction and analysis of riccionidin. Marchantia plants were grown on 1/100 Gamborg B5 medium with vitamins (Duchefa, Haarlem, The Netherlands) under a 16 h : 8 h, light : dark regime at 22° C for six weeks in order to induce production of riccionidin through nutrient deprivation. Riccionidin was extracted using MeOH : H_2O : HCl (1 : 1 : 0.02) in the ratio 1 : 1 (µl of extraction solution: mg of plant tissue, fresh weight). The samples were sonicated at room temperature for 15 min, centrifuged at 15,000 g and analyzed by HPLC-DAD-HRMS as described in Material and Methods. The samples were separated in a reverse phase column and analyzed in the positive ionization mode.

SDS gel and Western blot. SDS-PAGE analysis was performed according to Gutsche & Zachgo (2016). For each lane 3 µg protein was loaded. The gel was blotted onto a nitrocellulose membrane (Whatman, Maidstone, UK) and protein was detected using anti-MBP antibodies (NEB, Ipswich, MA, USA) and an anti-mouse antibody (Sigma-Aldrich, St. Louis, USA), conjugated to alkaline phosphatase. For visualization, NBT and BCIP were used as substrates, according to the manufacturer's instructions.

Expression analysis using semi-quantitative reverse transcription PCR. For expression analysis, total RNA isolation and cDNA synthesis were performed as described in Busch & Zachgo (2007). As a reference for normalization, constitutively expressed Mp*EF1α* was used. Semi-quantitative PCR was carried out at an annealing temperature of 60° C with 28 cycles for Mp*TCP1* and 18 for Mp*EF1α*. Averages and standard deviations are based upon two technical replicates. Gel bands were digitalized (Universal Hood II; Bio-Rad, Hercules, CA, USA) and quantified using the software Quantity One (Bio-Rad). Primer sequences are: Mp*TCP1* forward: ATGGGTGTGTGTGCCCCCTTGCCTGG, reverse: TTGGCGCGCCGGTAGTAGGTTTTAGTCATCTGACTG and Mp*EF1α* forward: TTCACTCGGGTGTGAAGCAG, reverse: GCCTCGAGTAAAGCTTCGTG.

Generation of genome–edited Mp*TCP1* knockout (Mp*tcp1*^{ge}) lines using the TALEN method. In order to underpin observed phenotypes generated with the double CRISPR/Cas9 approach, Mp*TCP1* knockout plants were generated with an alternative technique, the TALEN approach (Kopischke *et al.*, 2017). The TALEN target site within the TCP domain of Mp*TCP1* (Fig. S1a,c) was determined via tale-nt.cac.cornell.edu, selecting suitable sites in the target gene. The left (5′-TCGGACGGAGAGACCATAGA-3′) and right (5′-AGGCAGAACCTGCCATAATA-3′) TALEN arms were self-assembled with the FastTALE™ TALEN assembly kit from Sidansai Biotechnology as described by Kopischke *et al.* (2017). Both TALEN arms bind a 20 nt long target sequence separated by a 14 nt long spacer. The subsequent cloning in modified Marchantia binary expression vectors pMpGWB103 (left arm) and pMpGWB403 (right arm) was performed according to Kopischke *et al.* (2017). Transgenic T1 plants (lines Mp*tcp1-6*^{ge} - Mp*tcp1-10*^{ge}) were obtained via *Agrobacterium*-mediated sporeling transformation and confirmed by amplifying and sequencing a 1,797 nt long fragment including the TALEN target site (forward primer: ATGGGTGTGTGTGCCCCCTTGCCTGG, reverse primer: CATTCTGTACATTGTGCCGGCCTG).

Size measurement of 12 day-old Mp*tcp1*^{ge} TALEN lines. In order to measure surface areas, a minimum of 9 gemmae from six wild-type and five TALEN generated Mp*tcp1*^{ge} lines were cultivated as described in Material and Methods. Pictures were taken after 12 DAG with the Leica M165FC stereomicroscope with the mounted DFC490 camera (Leica,

Wetzlar, Germany) and surface areas of plants were measured using ImageJ. Values of each line were averaged.

RNA-Seq and H_2O_2 determination of archegoniophores. For total RNA isolation with subsequent RNA-Seq analysis and H_2O_2 determination using potassium iodide, wild-type archegoniophores were harvested with a maximal stalk length of 1 cm and a capitulum diameter of less than 3 mm. Mp*tcp1*^{ge} archegoniophores were harvested when outgrowth of secondary archegoniophores was not yet obvious. RNA isolation, RNA-Seq analysis (library preparation, sequencing and bioinformatics analysis) and H_2O_2 determination were performed as described in Material and Methods.

Treatment of gemmae with 3-AT. For 3-AT (3-amino-1,2,4-triazole) treatment, gemmae were grown either on ½ Gamborg B5 medium supplemented with 100 µM 3-AT or on medium without supplement (mock). For H_2O_2 determination, gemmae were grown for 9 days on either 3-AT supplemented or mock-medium containing 0.7% agar to facilitate gemmae extraction from medium. H_2O_2 determination and growth quantification was performed as described in Material and Methods.

References

Albert NW, Thrimawithana AH, McGhie TK, Clayton WA, Deroles SC, Schwinn KE, Bowman JL, Jordan BR, Davies KM. 2018. Genetic analysis of the liverwort *Marchantia polymorpha* reveals that R2R3MYB activation of flavonoid production in response to abiotic stress is an ancient character in land plants. *New Phytologist* **218**(2): 554-566.

Bowman JL, Kohchi T, Yamato KT, Jenkins J, Shu SQ, Ishizaki K, Yamaoka S, Nishihama R, Nakamura Y, Berger F, et al. 2017. Insights into Land Plant Evolution Garnered from the *Marchantia polymorpha* Genome. *Cell* **171**(2): 287-304.

Busch A, Zachgo S. 2007. Control of corolla monosymmetry in the Brassicaceae *Iberis amara*. *Proceedings of the National Academy of Sciences of the United States of America* **104**(42): 16714-16719.

Gutsche N, Zachgo S. 2016. The N-Terminus of the Floral Arabidopsis TGA Transcription Factor PERIANTHIA Mediates Redox-Sensitive DNA-Binding. *Plos One* **11**(4): e0153810.

Kopischke S, Schussler E, Althoff F, Zachgo S. 2017. TALEN-mediated genome-editing approaches in the liverwort *Marchantia polymorpha* yield high efficiencies for targeted mutagenesis. *Plant Methods* **13**. doi: 10.1186/s13007-017-0167-5

Kunz S, Burkhardt G, Becker H. 1994. Riccionidins A and B, anthocyanidins from the cell walls of the liverwort *Ricciocarpos natans*. *Phytochemistry* **35**(1): 233-235.

Tsuboyama S, Nonaka S, Ezura H, Kodama Y. 2018. Improved G-AgarTrap: A highly efficient transformation method for intact gemmalings of the liverwort *Marchantia polymorpha*. *Scientific Reports* **8**. doi: 10.1038/s41598-018-28947-0